New aspects of the inverse source problem with far-field data

Edwin A. Marengo

Department of Electrical and Computer Engineering, University of Arizona, Tucson, Arizona 85721

Anthony J. Devaney

Department of Electrical and Computer Engineering, Northeastern University, Boston, Massachusetts 02115

Richard W. Ziolkowski

Department of Electrical and Computer Engineering, University of Arizona, Tucson, Arizona 85721

Received October 26, 1998; accepted January 26, 1999

The time-dependent inverse source problem with far-field data is investigated within a limited-view Radon inversion framework, analogous to that of a limited-view computed tomography reconstruction problem. We investigate the domains in the Radon and Fourier spaces within which data are available for the reconstruction of the space–time structure of the source. Using a linear inversion formalism we derive a filtered backprojectionlike procedure to reconstruct the minimum-energy source consistent with prescribed far-field data. The source inversion technique developed in the paper is illustrated with a numerical example. The paper also contains a new description of nonradiating sources in the time domain. © 1999 Optical Society of America [S0740-3232(99)01507-0]

OCIS code: 100.3190.

1. INTRODUCTION

We consider the inhomogeneous wave equation

$$\left(\nabla^2 - \frac{1}{c^2}\frac{\partial^2}{\partial t^2}\right) U(\mathbf{r}, t) = -4\pi Q(\mathbf{r}, t), \tag{1}$$

where $Q(\mathbf{r}, t)$ is a radiating source localized within a simply connected spatial region D in three-dimensional (3D) space $\Re^3$ [such that $Q(\mathbf{r}, t) = 0$ for $\mathbf{r} \notin D$]. The (time-dependent) inverse source problem can be stated as being that of deducing $Q(\mathbf{r}, t)$ from knowledge of the radiated field[1]

$$U(\mathbf{r}, t) = \int_{-\infty}^{\infty} dt' \int d^3r' \frac{Q(\mathbf{r}', t')\delta\left(t' + \dfrac{|\mathbf{r} - \mathbf{r}'|}{c} - t\right)}{|\mathbf{r} - \mathbf{r}'|} \tag{2}$$

for all $\mathbf{r} \notin D$, for all times $t \in \Re$, where $\delta(\cdot)$ is Dirac's delta function. It is well known that the inverse source problem does not admit of a unique solution because of the existence, within the source's support D, of nonradiating (NR) sources, whose fields vanish for $\mathbf{r} \notin D$.[2–4]

It is easily deduced from Eq. (2) that the radiated field $U(\mathbf{r}, t)$ behaves as $U(r\mathbf{s}, t) \sim 1/rF(\mathbf{s}, \tau)$ as $r \to \infty$, where $\mathbf{s}$ is a unit vector specifying the observation direction, $\tau = t - r/c$, and

$$F(\mathbf{s}, \tau) = \int_{-\infty}^{\infty} dt' \int d^3r' Q(\mathbf{r}', t')\delta(t' - \mathbf{r}' \cdot \mathbf{s}/c - \tau). \tag{3}$$

Knowledge of the time-domain radiation pattern $F(\mathbf{s}, \tau)$ for all $\tau \in \Re$ and for all observation directions $\mathbf{s} \in S^2$, where S^2 is the unit sphere in $\Re^3$, completely determines $U(\mathbf{r}, t)$ everywhere outside D.[5] However, if the time-domain radiation pattern $F(\mathbf{s}, \tau)$ is known only for a discrete set of directions $\mathbf{s}$, one cannot, in general, uniquely determine $U(\mathbf{r}, t)$ for $\mathbf{r} \notin D$. Thus, the inverse source problem with far-field data, i.e., that of reconstructing a radiating source $Q(\mathbf{r}, t)$ of known spatial support D from knowledge of the time-domain radiation pattern $F(\mathbf{s}, \tau)$ for all retarded times τ and for a discrete or continuous set of observation directions $\mathbf{s}$, is seen to reduce to the inverse source problem as stated earlier only in the full view case wherein $F(\mathbf{s}, \tau)$ is known for all $\mathbf{s} \in S^2$.

In this paper the inverse source problem with far-field data is dealt with by using a limited-view Radon inversion framework, analogous to that of a limited-view computed tomography (CT) reconstruction problem.[6,7] Our motivation is twofold: (a) that of synthesizing the minimum L^2 norm [minimum-energy (ME)] source, of specified spatial support, that generates a prescribed far field and (b) that of reconstructing an unknown source from field data gathered in the far-zone region of the source (e.g., a source/target interrogation application). Whereas in (a) the far field can be prescribed for all $\mathbf{s} \in S^2$, in (b) far-field data are available only for a discrete set of observation directions. Also, whereas application (a) can involve noise-free data, i.e., in the space of realizable far fields (see, e.g., Yaghjian and Hansen[8] and Friedlander,[9]) application (b) involves noisy data. The former problem

0740-3232/99/071612-11$15.00

will admit of an *exact* ME solution (i.e., the normal solution[10]), whereas the latter will have an *approximate* ME solution (i.e., the normal pseudosolution[10]).

The inverse source problem has been studied in the frequency domain by many authors, for both scalar[4,11] and electromagnetic[2] sources. The first treatment of the electromagnetic inverse source problem in the time domain appears to be due to Moses,[12] who addressed both the nonuniqueness question and *a priori* constraints that may render the inverse source problem unique. In Ref. 13, the same author explores inverse initial-value problems for the wave equation and Maxwell's equations. Most of the analysis in Refs. 12 and 13, although of the most importance, applies only to sources with a certain separable space–time dependence. The solutions in Refs. 12 and 13 are not, in general, ME solutions.

The remainder of the paper is organized as follows. In Section 2 we review the direct (radiation) problem and investigate the domains in the Radon and Fourier spaces within which data are available for the reconstruction of the space–time structure of the source. In Subsection 3.A we derive—by using standard methods of linear inversion theory—a new filtered backprojectionlike procedure to reconstruct the ME source $Q_{\mathrm{ME}}(\mathbf{r}, t)$, of known spatial support D, that generates a prescribed time-domain radiation pattern $F(\mathbf{s}, \tau)$ known for all τ and for a discrete or continuum set of observation directions $\mathbf{s}$. The reconstruction technique is developed analytically in Subsection 3.B by means of spherical harmonics and is illustrated in Subsection 3.C with a numerical example. In Section 4 we present a new description of NR sources in the time domain that makes use of results on time-dependent multipoles derived in Ref. 5. In the final part of Section 4 we derive an orthogonality relation between NR sources and solutions of the homogeneous wave equation that leads to a new definition of NR sources in the time domain. Section 5 contains our concluding remarks.

The work in Section 3 represents a new treatment of the scalar inverse source problem with far-field data through pseudoinversion of limited-view Radon-transform operators. The approach is similar to that in Ref. 14, where a regularized pseudoinverse technique is applied to ground-penetrating-radar imaging. The discussion in Sections 3 and 4 sheds new light into the properties of ME and NR sources in the time domain.

2. THE DIRECT PROBLEM

On introducing the source function $\rho(\boldsymbol{\mathcal{X}}) \equiv Q(\mathbf{r}, t)$ where $\boldsymbol{\mathcal{X}} = (\mathcal{X}_0 = ct, \mathcal{X}_1 = x, \mathcal{X}_2 = y, \mathcal{X}_3 = z)$, one obtains from Eq. (3)

$$F(\mathbf{s}, \tau) = \frac{1}{\sqrt{2}} \int \mathrm{d}^4\mathcal{X} M(\boldsymbol{\mathcal{X}}) \rho(\boldsymbol{\mathcal{X}}) \delta(c\tau/\sqrt{2} - \boldsymbol{\mathcal{X}} \cdot \boldsymbol{\mathcal{V}}_{\mathbf{s}}), \tag{4}$$

where

$$\boldsymbol{\mathcal{V}}_{\mathbf{s}} = \left(\mathcal{V}_{\mathbf{s}0} = \frac{1}{\sqrt{2}}, \quad \mathcal{V}_{\mathbf{s}1} = -\frac{1}{\sqrt{2}} s_x, \quad \mathcal{V}_{\mathbf{s}2} = -\frac{1}{\sqrt{2}} s_y, \right.$$

$$\left. \mathcal{V}_{\mathbf{s}3} = -\frac{1}{\sqrt{2}} s_z \right), \tag{5}$$

where $\mathbf{s} = (s_x, s_y, s_z)$ and $M(\boldsymbol{\mathcal{X}})$ is a masking function defined by

$$M(\boldsymbol{\mathcal{X}}) = \begin{cases} 1 & \text{if } \boldsymbol{\mathcal{X}} \in \mathcal{D} \\ 0 & \text{otherwise} \end{cases}, \tag{6}$$

where $\mathcal{D}$ is a space–time region where the source is known to be confined. For example, later in the paper we will consider sources that are spatially localized within two concentric spheres with center at the origin and radii $r \equiv |\mathbf{r}| = a$ and b, respectively, with $b < a$, so that

$$M(\boldsymbol{\mathcal{X}}) = \begin{cases} 1 & \text{if } b \leqslant r \leqslant a \\ 0 & \text{otherwise} \end{cases}. \tag{7}$$

For $b = 0$ the masking function in Eq. (7) reduces to that for a source that is known to be confined within the spherical volume $V: r \leqslant a$.

The fourfold Radon transform $(\mathcal{R}\rho)(\boldsymbol{\mathcal{V}}, \xi)$ of $\rho(\boldsymbol{\mathcal{X}})$ corresponding to the hyperplane $\boldsymbol{\mathcal{X}} \cdot \boldsymbol{\mathcal{V}} - \xi = 0$, where $\boldsymbol{\mathcal{V}}$ is a unit vector in the four-dimensional (4D) Radon domain (defining the orientation of the hyperplane) and ξ is a real parameter (defining the distance of the hyperplane to the origin), is defined as[15]

$$(\mathcal{R}\rho)(\boldsymbol{\mathcal{V}}, \xi) = \int \mathrm{d}^4\mathcal{X} \rho(\boldsymbol{\mathcal{X}}) \delta(\xi - \boldsymbol{\mathcal{X}} \cdot \boldsymbol{\mathcal{V}}). \tag{8}$$

The time-domain radiation pattern $F(\mathbf{s}, \tau)$ is identified from Eqs. (4) and (8) as being equal to the fourfold Radon transform of $\rho(\boldsymbol{\mathcal{X}})$ evaluated at the hyperplane $\boldsymbol{\mathcal{X}} \cdot \boldsymbol{\mathcal{V}}_{\mathbf{s}} - c\tau/\sqrt{2} = 0$ (apart from a factor $1/\sqrt{2}$). For fixed $\mathbf{s}$ and as a function of τ alone, $F(\mathbf{s}, \tau)$ is given by the projection of $\rho(\boldsymbol{\mathcal{X}})$ onto the line in the direction of the unit vector $\boldsymbol{\mathcal{V}}_{\mathbf{s}}$. (A projection of a multidimensional function onto a line is the integral of this function over hyperplanes that are perpendicular to the given line). Figure 1(a) depicts a schematization of the 3D space–time counterpart of Eq. (4) [where $\boldsymbol{\mathcal{X}} = (\mathcal{X}_0 = ct, \mathcal{X}_1 = x, \mathcal{X}_2 = y)$], illustrating the relationship between $\mathbf{s}$ and $\boldsymbol{\mathcal{V}}_{\mathbf{s}}$ and the line in the direction of the unit vector $\boldsymbol{\mathcal{V}}_{\mathbf{s}}$ along which the projections are computed. For prescribed $F(\mathbf{s}, \tau)$, data to recover $\rho(\boldsymbol{\mathcal{X}})$ are thus seen from Eq. (4) to consist of Radon projections along radial lines (in the 4D Radon domain) tangent to a generalized cone with apex at the origin, i.e., the light cone.[1] Figure 1(b) illustrates the light cone in 3D space–time. Radon projections onto directions outside the light cone cannot be inferred from $F(\mathbf{s}, \tau)$, making the inversion nonunique. The inverse source problem with far-field data reduces to finding source functions consistent with Radon projections provided *only* for directions that lie tangentially on the surface of the light cone [NR sources are those whose Radon projections onto those directions vanish (see Section 4)]. This is analogous to a limited-view CT reconstruction problem, where Radon projections of an object are provided only for a limited number of directions.[6,7]

The frequency-domain radiation pattern $f(\mathbf{s}, \omega) \equiv \int_{-\infty}^{\infty} \mathrm{d}\tau \exp(i\omega\tau) F(\mathbf{s}, \tau)$ is found from Eq. (4) to be

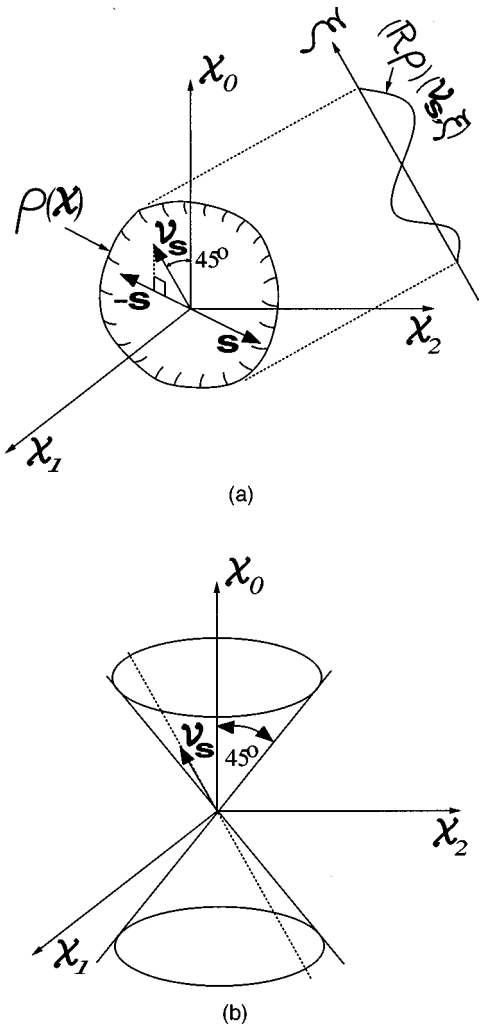

Fig. 1. (a) Schematization of $\rho(\boldsymbol{\mathcal{X}})$ and its Radon projection $(R\rho)(\boldsymbol{\mathcal{V}}_{\mathbf{s}}, \xi)$ in a viewing direction $\boldsymbol{\mathcal{V}}_{\mathbf{s}}$, showing the relationship between $\boldsymbol{\mathcal{V}}_{\mathbf{s}}$, $\mathbf{s}$, and the rotated coordinate axis ξ used in the definition of the Radon transform in 3D space–time. (b) The light cone in 3D space–time.

$$f(\mathbf{s}, \omega) = \frac{1}{c}\int \mathrm{d}^4\mathcal{X} M(\boldsymbol{\mathcal{X}})\rho(\boldsymbol{\mathcal{X}})\exp\left(i\frac{\sqrt{2}\omega}{c}\boldsymbol{\mathcal{V}}_{\mathbf{s}}\cdot\boldsymbol{\mathcal{X}}\right). \quad (9)$$

It is given by the fourfold (spatial–temporal) Fourier transform of the masked source evaluated at points over the surface of a generalized cone in the 4D Fourier domain $(\omega/c, \mathbf{k})$ (where $\mathbf{k}$ is the spatial-frequency vector) centered at the origin $(\omega/c = 0, \mathbf{k} = 0)$. We see that while $F(\mathbf{s}, \tau)$ provides information about Radon projections of $\rho(\boldsymbol{\mathcal{X}})$ *only* along lines tangent to the light cone (see Fig. 1), $f(\mathbf{s}, \omega)$ provides information about the fourfold Fourier transform of $\rho(\boldsymbol{\mathcal{X}})$ *only* over the surface of an analogous generalized cone in the 4D Fourier domain. Thus $f(\mathbf{s}, \omega)$ alone is insufficient to uniquely determine $\rho(\boldsymbol{\mathcal{X}})$ through Fourier inversion, confirming the nonunique nature of the inverse source problem.

3. SOURCE INVERSION FROM FAR-FIELD DATA

We derive below the ME [minimum L^2 norm $\int \mathrm{d}^4\mathcal{X}|\rho(\boldsymbol{\mathcal{X}})|^2$] solution $\rho_{\mathrm{ME}}(\boldsymbol{\mathcal{X}}) \equiv Q_{\mathrm{ME}}(\mathbf{r}, t)$ to the inverse source problem with far-field data. The method applies to cases involving either full- or limited-view far-field data as long as one uses integration $\int_{S^2}\mathrm{d}\mathbf{s}$ in the former or summation $\Sigma_{\mathbf{s}}$ over available directions $\mathbf{s}$ in the latter. For the sake of brevity, we shall use the notation $\int_{S^2}\mathrm{d}\mathbf{s}$ for either case. The general formulation is presented in Subsection 3.A and developed further in Subsection 3.B for the special case of sources characterized by the masking function in Eq. (7). A numerical example based on the general results in Subsection 3.A is given in Subsection 3.C.

A. General Formulation

First we write Eq. (4) in the form of a linear mapping

$$F = P\rho, \quad (10)$$

where $\rho(\boldsymbol{\mathcal{X}}) \in X$; where $X = L^2(\Re^4)$ is the Hilbert space of L^2 functions of $\boldsymbol{\mathcal{X}} \in \Re^4$, $F(\mathbf{s}, \tau) \in Y$; where Y is the Hilbert space formed from the direct product of the space of L^2 functions of $\tau \in \Re$ with the space of L^2 functions of $\mathbf{s} \in S^2$; and $P{:}X \to Y$ is a linear transform mapping the space X into the space Y. The inner products in the Hilbert spaces defined above are defined in the usual way. For example, for $\rho_1(\boldsymbol{\mathcal{X}}) \in X$, $\rho_2(\boldsymbol{\mathcal{X}}) \in X$,

$$\langle \rho_1, \rho_2\rangle_X = \int d^4\mathcal{X}\rho_1^*(\boldsymbol{\mathcal{X}})\rho_2(\boldsymbol{\mathcal{X}}),$$

where * denotes the complex conjugate.

The adjoint $P^\dagger$ of P, defined by

$$\langle F, P\rho\rangle_Y = \langle P^\dagger F, \rho\rangle_X,$$

is found from Eq. (4) to be

$$(P^\dagger F)(\boldsymbol{\mathcal{X}}) = M(\boldsymbol{\mathcal{X}})\frac{1}{c}\int_{S^2}\mathrm{d}\mathbf{s}F(\mathbf{s}, \sqrt{2}\boldsymbol{\mathcal{V}}_{\mathbf{s}}\cdot\boldsymbol{\mathcal{X}}/c). \quad (11)$$

The operation associated with $P^\dagger$ is that of backprojection.[16] The masking function $M(\boldsymbol{\mathcal{X}})$ guarantees that $P^\dagger$ maps $Y \to X$. Then the operators $PP^\dagger$ and $P^\dagger P$ map $Y \to Y$ and $X \to X$, respectively. In rewriting Eq. (11) in the form

$$(P^\dagger F)(\boldsymbol{\mathcal{X}}) = M(\boldsymbol{\mathcal{X}})\frac{1}{c}\int_{S^2}\mathrm{d}\mathbf{s}F(\mathbf{s}, t - \mathbf{s}\cdot\mathbf{r}/c), \quad (12)$$

we see that $(P^\dagger F)(\boldsymbol{\mathcal{X}})$ is given by the product of the masking function with a superposition of time-dependent plane waves whose amplitudes are determined by $F(\mathbf{s}, \tau)$. In particular, $(P^\dagger F)(\boldsymbol{\mathcal{X}})$ is defined by a free-field plane-wave expansion truncated within $\mathcal{D}$. Then $(P^\dagger F)(\boldsymbol{\mathcal{X}})$ obeys the homogeneous wave equation

$$\left(\nabla^2 - \frac{1}{c^2}\frac{\partial^2}{\partial t^2}\right)(P^\dagger F)(\boldsymbol{\mathcal{X}}) = 0, \quad (13)$$

in the interior of the domain $\mathcal{D}$, its boundary excluded.

The unique solution with minimum L^2 norm to the inverse problem Eq. (10) is[16,17]

$$\rho_{\mathrm{ME}}(\boldsymbol{\mathcal{X}}) = (P^\dagger\bar{F})(\boldsymbol{\mathcal{X}}), \quad (14)$$

where $\bar{F}(\mathbf{s}, \tau)$ is the filtered time-domain radiation pattern defined by

$$(PP^{\dagger}\bar{F})(\mathbf{s}, \tau) = F(\mathbf{s}, \tau). \tag{15}$$

If the far-field data are noise free [i.e., $F(\mathbf{s}, \tau) \in R(P)$, where $R(P) = \{F \in Y: F = P\rho, \rho \in X\}$ is the range of P], then expressions (14) and (15) define the normal solution to the inverse source problem. When dealing with noisy data or if the solution to Eq. (10) is unstable, the method of Tikhonov–Phillips regularization (or any other regularization method[17]) can be used to generate approximate ME solutions to Eq. (10) (see, e.g., Ref. 14). For example, the Tikhonov–Phillips regularized pseudoinverse-based solution is

$$\rho_{\mathrm{ME}} = P^{\dagger}[PP^{\dagger} + \beta I]^{-1}F, \tag{16}$$

where I is the identity operator and β is the Tikhonov–Phillips regularization parameter, whose value is determined by a trade-off between accuracy and computational stability.[14] As $\beta \to 0$, the approximate solution Eq. (16) approaches the least-squares solution of minimum L^2 norm (i.e., the normal pseudosolution).

It follows from Eqs. (13) and (14) that

$$\left(\nabla^2 - \frac{1}{c^2}\frac{\partial^2}{\partial t^2}\right)\rho_{\mathrm{ME}}(\boldsymbol{\mathcal{X}}) = 0 \tag{17}$$

in the interior of the domain $\mathcal{D}$, its boundary excluded. The frequency-domain analog of this result, i.e., that the temporal Fourier transform of ME sources of spatial support D obey—for fixed frequency ω—the homogeneous Helmholtz equation inside D, is implicit in treatments of the inverse source problem by Bleistein and Cohen,[2] Devaney and Porter,[4] and Porter and Devaney.[18] However, this property of ME sources appears to have received little attention.

For a time-independent masking function $M(\boldsymbol{\mathcal{X}}) = M(\mathbf{r})$, we obtain from Eqs. (4) and (11) the following result, applicable to cases involving perfect (noise-free) data:

$$\begin{aligned}(PP^{\dagger}\bar{F})(\mathbf{s}, \tau) &= \frac{1}{c}\int \mathrm{d}t' \int \mathrm{d}^3r' M(\mathbf{r}')\delta(\tau + \mathbf{r}' \cdot \mathbf{s}/c - t') \\ &\quad \times \int_{S^2} \mathrm{d}\mathbf{s}' \bar{F}(\mathbf{s}', t' - \mathbf{r}' \cdot \mathbf{s}'/c) \\ &= \frac{1}{c}\int_{S^2} \mathrm{d}\mathbf{s}' \int \mathrm{d}t'' \bar{F}(\mathbf{s}', t'') \int \mathrm{d}^3r' M(\mathbf{r}') \\ &\quad \times \delta[t'' - \tau - \mathbf{r}' \cdot (\mathbf{s} - \mathbf{s}')/c] \\ &= \frac{1}{c}\int_{S^2} \mathrm{d}\mathbf{s}' \bar{F}(\mathbf{s}', \tau) \otimes h(\mathbf{s} - \mathbf{s}', \tau),\end{aligned} \tag{18}$$

where $\otimes$ denotes temporal convolution and

$$h(\mathbf{s} - \mathbf{s}', \tau) = \int \mathrm{d}^3r' M(\mathbf{r}')\delta[\tau + (\mathbf{s} - \mathbf{s}') \cdot \mathbf{r}'/c]. \tag{19}$$

It follows from Eqs. (15) and (18) that

$$\frac{1}{c}\int_{S^2} \mathrm{d}\mathbf{s}' \bar{F}(\mathbf{s}', \tau) \otimes h(\mathbf{s} - \mathbf{s}', \tau) = F(\mathbf{s}, \tau). \tag{20}$$

As a function of $\mathbf{s}$ and τ for fixed $\mathbf{s}'$, the quantity $h(\mathbf{s} - \mathbf{s}', \tau)$ in Eq. (19) is identified from Eq. (4) as being the time-domain radiation pattern of a uniformly distributed source whose support is specified by $M(\mathbf{r})$, impulsively excited (pulsed) with a progressive time delay $\mathbf{r} \cdot \mathbf{s}'/c$, i.e., a source of the space–time-separable form

$$Q(\mathbf{r}, t) = M(\mathbf{r})\delta(t - \mathbf{r} \cdot \mathbf{s}'/c). \tag{21}$$

A detailed analysis of the class of sources defined by Eq. (21) is given in Refs. 19 and 20 with $\mathbf{s}'$ playing the role of the main beam axis in those papers. Equation (20) states that the unfiltered data $F(\mathbf{s}, \tau)$ are equal to the sum over all available directions $\mathbf{s}'$ of the time-domain radiation pattern of a source that consists of a uniform distribution of point radiators (within the spatial support of the sought-after source) all of which are excited, with a progressive time delay $\mathbf{r} \cdot \mathbf{s}'/c$, by the same time signature, the latter being precisely—for a given $\mathbf{s}'$—the time signature of the filtered data $\bar{F}(\mathbf{s}', \tau)$. In other words, for each direction $\mathbf{s}'$, the filtered data $\bar{F}(\mathbf{s}', \tau)$ can be thought of as the excitation signals that one must apply at each point of an imaginary, uniform source distribution of the form of Eq. (21) in order to obtain, by summing up the time-domain radiation patterns associated with these sources (i.e., for all available directions $\mathbf{s}$), the original data $F(\mathbf{s}, \tau)$.

Equation (20) must be inverted to compute the ME source by means of Eqs. (11) and (14). This can be accomplished by taking the one-dimensional Fourier transform of the available Radon projections of the source with respect to the radial parameter in the definition of the Radon transform (i.e., the temporal variable $c\tau/\sqrt{2}$) in a manner analogous to the use of the projection-slice theorem in the filtered backprojection algorithm or the Fourier interpolation methods of CT (Ref. 21). By temporally Fourier transforming both sides of Eqs. (19) and (20), one obtains

$$\frac{1}{c}\int_{S^2} \mathrm{d}\mathbf{s}' \tilde{f}(\mathbf{s}', \omega)\tilde{h}(\mathbf{s} - \mathbf{s}', \omega) = f(\mathbf{s}, \omega), \tag{22}$$

where

$$\tilde{h}(\mathbf{s} - \mathbf{s}', \omega) = \int \mathrm{d}^3r' M(\mathbf{r}') \exp\left[-i\frac{\omega}{c}\mathbf{r}' \cdot (\mathbf{s} - \mathbf{s}')\right]. \tag{23}$$

We are now in position to evaluate the ME solution via the following steps:

1. Solve the filtering operation [Eq. (22)] (either numerically or analytically).
2. Recover the filtered data $\bar{F}(\mathbf{s}, \tau)$ from $\tilde{f}(\mathbf{s}, \omega)$ via temporal Fourier inversion.
3. Backproject the filtered data $\bar{F}(\mathbf{s}, \tau)$ with Eq. (11), as is required by the reconstruction formula [Eq. (14)].

Other CT reconstruction methods, potentially applicable to the inverse source problem with far-field data but not to be considered here, are iterative in nature and include the algebraic reconstruction technique and the simultaneous iterative reconstruction technique.[21]

The quantity $\bar{h}(\mathbf{s}-\mathbf{s}', \omega)$ in Eq. (23) is the frequency-domain radiation pattern of an impulsively excited source of the form of Eq. (21). Closed-form expressions for $\tilde{h}(\mathbf{s}-\mathbf{s}', \omega)$ for canonical source geometries given in Refs. 19 and 20 can be used to solve integral equation (22) numerically (see, e.g., the numerical procedure used in Ref. 14). This is the procedure employed in the numerical example in Subsection 3.C. In Subsection 3.B we solve, by means of spherical harmonics, the filtering operation [Eq. (22)] analytically for sources characterized by the masking function in Eq. (7).

B. Spherical-Harmonics Expansion Solution

The method developed in this section assumes that the far fields are known for all $\mathbf{s} \in S^2$; the method applies to sources characterized by masking functions with radial dependence only, i.e., such that $M(\mathbf{r}) = M(r)$. We will consider sources localized within two concentric spheres with center at the origin and radii $r = a$ and b, with $b < a$ [masking function defined by Eq. (7)]. For the case of a source that fills the whole spherical volume V: $r \leqslant a$, we have $b = 0$.

Starting with the multipole expansion of the plane wave,[1]

$$\exp\left(i\frac{\omega}{c}r'\hat{\mathbf{r}}'\cdot\mathbf{s}\right) = 4\pi\sum_{l=0}^{\infty}\sum_{m=-l}^{l} i^l j_l\left(\frac{\omega}{c}r'\right)Y_{l,m}(\hat{\mathbf{r}}')Y_{l,m}^*(\mathbf{s}), \quad (24)$$

where $\hat{\mathbf{r}}' \equiv \mathbf{r}'/r'$, $j_l(\cdot)$ is the spherical Bessel function of the first kind and order l, and $Y_{l,m}(\hat{\mathbf{r}})$ is the spherical harmonic of degree l and order m (as defined in Ref. 1, p. 99), Eq. (23) reduces—in view of the orthogonality of the spherical harmonics—to

$$\tilde{h}(\mathbf{s}-\mathbf{s}', \omega) = \sum_{l=0}^{\infty}\sum_{m=-l}^{l}\sigma_l^2(\omega)Y_{l,m}(\mathbf{s})Y_{l,m}^*(\mathbf{s}'), \quad (25)$$

where

$$\sigma_l^2(\omega) = (4\pi)^2\int_b^a \mathrm{d}r' r'^2 j_l^2\left(\frac{\omega}{c}r'\right) = \alpha_l^2(\omega) - \beta_l^2(\omega), \quad (26)$$

where

$$\alpha_l^2(\omega) = 8\pi^2 a^3\left[j_l^2\left(\frac{\omega}{c}a\right) - j_{l-1}\left(\frac{\omega}{c}a\right)j_{l+1}\left(\frac{\omega}{c}a\right)\right], \quad (27)$$

$$\beta_l^2(\omega) = 8\pi^2 b^3\left[j_l^2\left(\frac{\omega}{c}b\right) - j_{l-1}\left(\frac{\omega}{c}b\right)j_{l+1}\left(\frac{\omega}{c}b\right)\right]. \quad (28)$$

In evaluating $\sigma_l^2(\omega)$ we have made use of the second Lommel integral (see Ref. 22, p. 594) and the recurrence relations for the Bessel functions (see, e.g., Ref. 22, p. 576–578). For $b = 0$ we obtain $\sigma_l^2(\omega) = \alpha_l^2(\omega)$. The singular values corresponding to this special case will be used for normalization purposes later.

We expand $f(\mathbf{s}, \omega)$ and $\bar{f}(\mathbf{s}, \omega)$ as series of spherical harmonics; i.e.,

$$f(\mathbf{s}, \omega) = \sum_{l=0}^{\infty}\sum_{m=-1}^{l}(-i)^l\tilde{a}_{l,m}(\omega)Y_{l,m}(\mathbf{s}),$$

$$\bar{f}(\mathbf{s}, \omega) = \sum_{l=0}^{\infty}\sum_{m=-1}^{l}(-i)^l\tilde{\bar{a}}_{l,m}(\omega)Y_{l,m}(\mathbf{s}), \quad (29)$$

where

$$\tilde{a}_{l,m}(\omega) = i^l\int_{S^2}\mathrm{d}\mathbf{s} f(\mathbf{s}, \omega)Y_{l,m}^*(\mathbf{s}),$$

$$\tilde{\bar{a}}_{l,m}(\omega) = i^l\int_{S^2}\mathrm{d}\mathbf{s}\bar{f}(\mathbf{s}, \omega)Y_{l,m}^*(\mathbf{s}). \quad (30)$$

If we now make use of Eq. (25), we can solve integral equation (22). We find that

$$\tilde{a}_{l,m}(\omega) = \frac{1}{c}\sigma_l^2(\omega)\tilde{\bar{a}}_{l,m}(\omega), \quad (31)$$

which corresponds to the filtering operation in the filtered backprojection algorithm.

Finally, by Fourier transforming to the time-domain expressions (29)–(31), one solves for the filtered data $\bar{F}(\mathbf{s}, \tau)$, which can be then backprojected according to Eqs. (11) and (12). This procedure yields

$$\begin{aligned} Q_{\mathrm{ME}}(\mathbf{r}, t) &= M(\mathbf{r})\frac{1}{2\pi}\int_{-\infty}^{\infty}\mathrm{d}\omega\exp(-i\omega t) \\ &\quad\times\sum_{l=0}^{\infty}\sum_{m=-l}^{l}4\pi\tilde{a}_{l,m}(\omega)\sigma_l^{-2}(\omega)j_l\left(\frac{\omega}{c}r\right)Y_{l,m}(\hat{\mathbf{r}}) \\ &= \frac{1}{2\pi}\int_{-\infty}^{\infty}\mathrm{d}\omega\exp(-i\omega t)\int_{S^2}\mathrm{d}\mathbf{s} f(\mathbf{s}, \omega)\tilde{H}(\mathbf{r}, \mathbf{s}, \omega) \\ &= \int_{S^2}\mathrm{d}\mathbf{s} F(\mathbf{s}, t)\otimes H(\mathbf{r}, \mathbf{s}, t), \end{aligned} \quad (32)$$

where we have made use of Eq. (24) and where we have defined

$$\tilde{H}(\mathbf{r}, \mathbf{s}, \omega) = 4\pi M(\mathbf{r})\sum_{l=0}^{\infty}\sum_{m=-l}^{l} i^l\sigma_l^{-2}(\omega)j_l\left(\frac{\omega}{c}r\right)Y_{l,m}(\hat{\mathbf{r}})Y_{l,m}^*(\mathbf{s}),$$

$$H(\mathbf{r}, \mathbf{s}, t) = 2M(\mathbf{r})\int_{-\infty}^{\infty}\mathrm{d}\omega\exp(-i\omega t) \times\sum_{l=0}^{\infty}\sum_{m=-1}^{l} i^l\sigma_l^{-2}(\omega)j_l\left(\frac{\omega}{c}r\right)Y_{l,m}(\hat{\mathbf{r}})Y_{l,m}^*(\mathbf{s}). \quad (33)$$

Thus the ME solution to the inverse source problem is given by convolution integral Eq. (32), where the quantity $H(\mathbf{r}, \mathbf{s}, t)$ plays the role of impulse response (for source inversion of the ME source contribution only).

The L^2 norm of the ME solution $Q_{\mathrm{ME}}(\mathbf{r}, t)$ is found from Eq. (32) to be

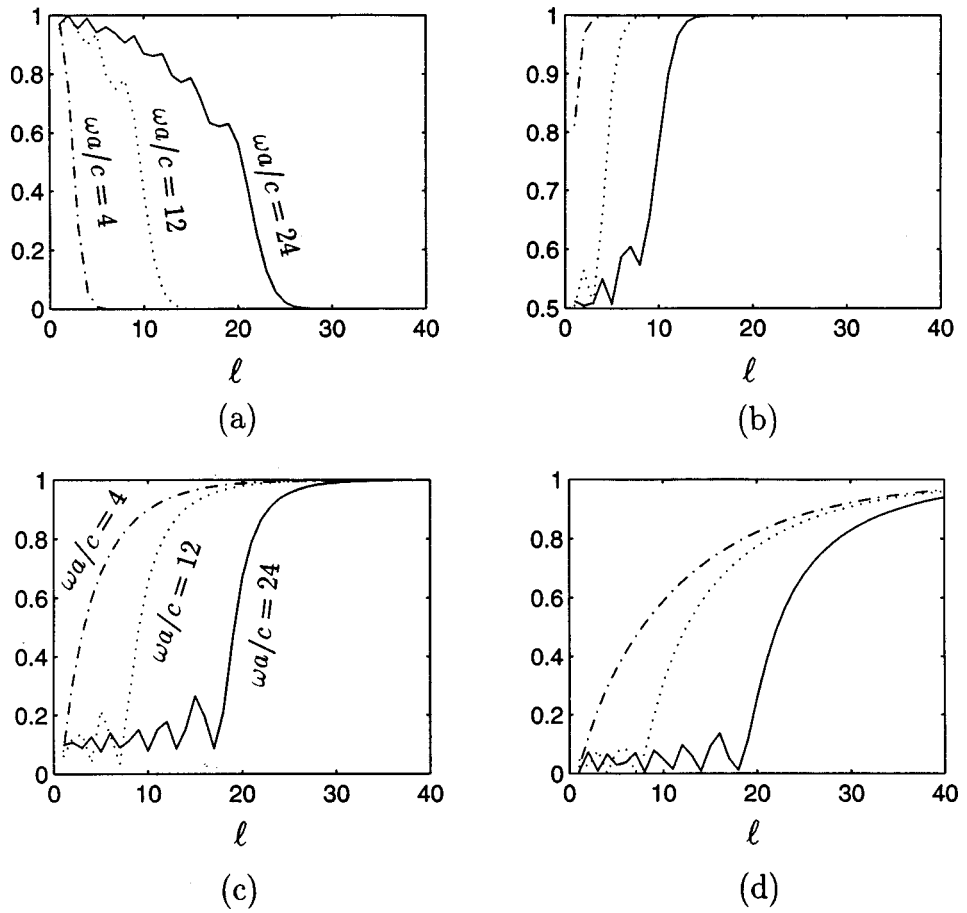

Fig. 2. (a) Plots of the normalized singular values $\bar{\sigma}_l^2$ versus l and parameterized by $\omega a/c$ for a source in the spherical volume V:$r \leqslant a$. (b)–(d) Plots of $\sigma_l^2(\omega)/\alpha_l^2(\omega)$ versus l and parameterized by $\omega a/c$ for sources in the spherical shells defined by $b \leqslant r \leqslant a$ with $b = 0.5a$, $b = 0.9a$ and $b = 0.97a$, respectively.

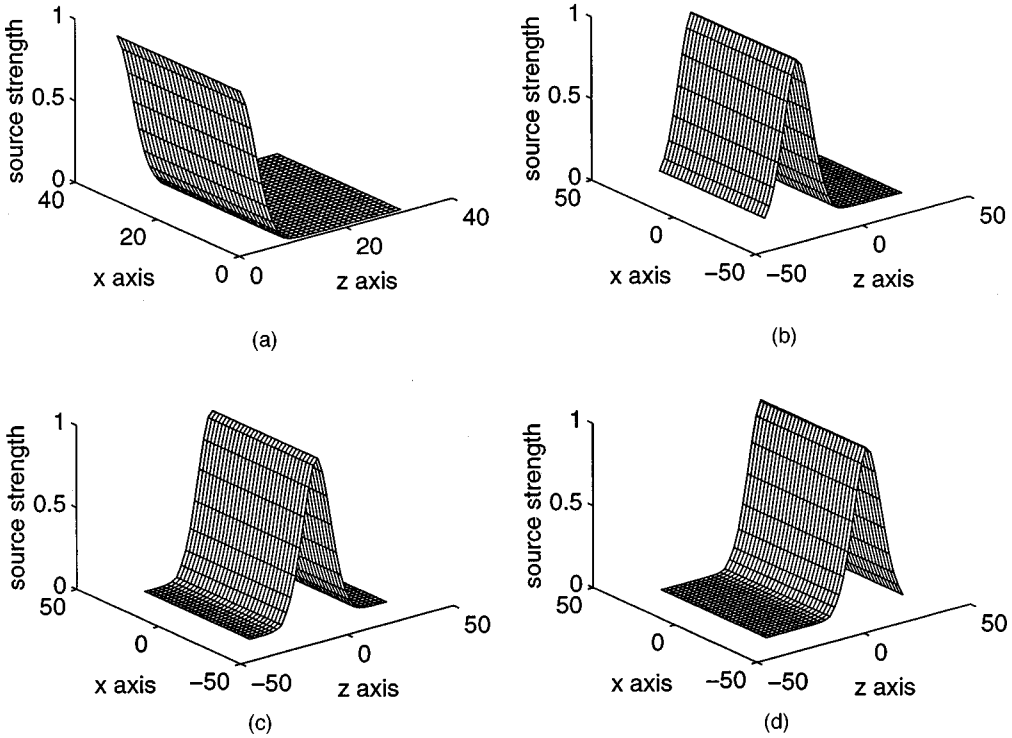

Fig. 3. Source spatial profile at different times.

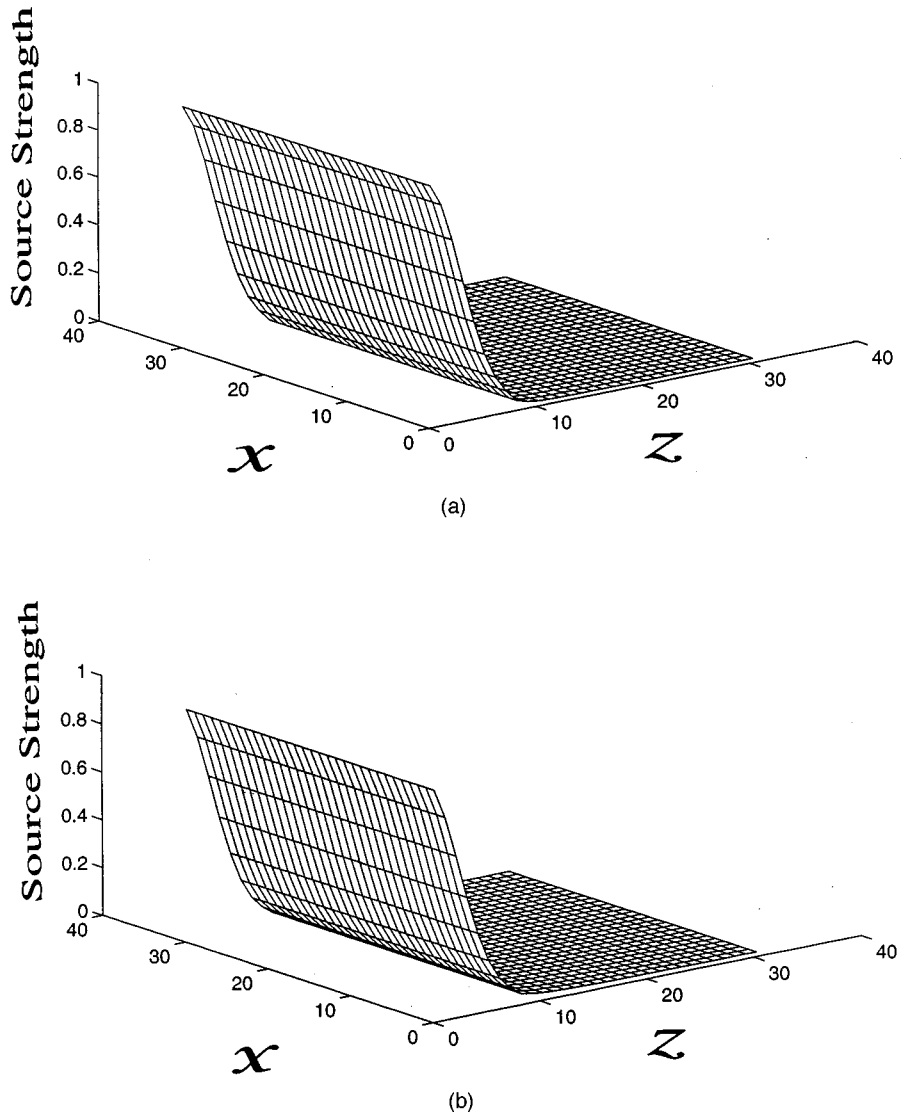

Fig. 4. Results for the time in Fig. 3(a): (a) original source spatial profile, (b) reconstructed source spatial profile obtained from the filtered backprojection algorithm.

$$\int_{-\infty}^{\infty} dt \int_D d^3r |Q_{\mathrm{ME}}(\mathbf{r}, t)|^2 = \frac{1}{2\pi} \int_{-\infty}^{\infty} d\omega \sum_{l=0}^{\infty} \sum_{m=-l}^{l} |\tilde{a}_{l,m}(\omega)|^2 \sigma_l^{-2}(\omega). \quad (34)$$

Plots of the normalized singular values $\bar{\sigma}_l^2(\omega) \equiv \sigma_l^2(\omega)/\alpha_l^2(0)$ versus l and parameterized by $\omega a/c$ for a source in the spherical volume V [where $b = 0$ and $\sigma_l^2(\omega) = \alpha_l^2(\omega)$] are given in Fig. 2(a). Plots of $\sigma_l^2(\omega)/\alpha_l^2(\omega)$ versus l and parameterized by $\omega a/c$ are given in Figs. 2(b), 2(c) and 2(d), for the cases $b = 0.5a$, $b = 0.9a$, and $b = 0.97a$ (a thin spherical shell), respectively. The plots in Figs. 2(a) and 2(d) show that the singular values $\sigma_l^2(\omega)$ corresponding to the case of a thin spherical shell (quasi-spherical surface) decay more rapidly with l than those for the case of a fully spherical volume where $b = 0$. Thus it appears in view of Eq. (34) that ME solutions to the inverse source problem that fill the whole spherical volume V are, in general, more efficient than equivalent quasi-surface sources in the vicinity of the boundary $r = a$ in radiating prescribed fields outside V. In all cases considered, the normalized singular values $\bar{\sigma}_l^2(\omega)$ are seen to decay rapidly for $l \gtrsim \omega a/c$, confirming ill-conditioning [see Ref. 18 for a detailed account of the properties of $\alpha_l^2(\omega)$]. It follows that in order to make practical use of Eqs. (32) and (33), one must truncate the spherical harmonics expansion in Eq. (32) so as to enforce the stability requirement $l \lesssim \omega a/c$.

C. Numerical Illustration

We present below the results of computer simulations in two-dimensional space. We considered a uniformly distributed source $Q(\mathbf{r}, t)$ of the form

$$Q(\mathbf{r}, t) = M(\mathbf{r}) G(t - \hat{\mathbf{z}} \cdot \mathbf{r}/c) \quad (35)$$

spatially confined in (x, z) space within the rectangular region $\{\mathbf{r} \in \Re^2 : |x| \leq a_x/2, |z| \leq a_z/2\}$ (i.e., $M = 1$ inside this region and $M = 0$ elsewhere), so that from Eqs. (22) and (23),

$$\tilde{h}(\mathbf{s}-\mathbf{s}',\omega)=\tilde{h}(\phi,\phi',\omega)$$
$$=a_x a_z \operatorname{sinc}\left[\frac{\omega a_x}{2c}(s_x-s_x')\right]\times\operatorname{sinc}\left[\frac{\omega a_z}{2c}(s_z-s_z')\right]$$
$$=a_x a_z \operatorname{sinc}\left[\frac{\omega a_x}{2c}(\sin\phi-\sin\phi')\right]\times\operatorname{sinc}\left[\frac{\omega a_z}{2c}(\cos\phi-\cos\phi')\right], \quad (36)$$

where $\operatorname{sinc}(\cdot)=\sin(\cdot)/(\cdot)$ and where $\mathbf{s}=\sin\phi\hat{\mathbf{x}}+\cos\phi\hat{\mathbf{z}}$ and $\mathbf{s}'=\sin\phi'\hat{\mathbf{x}}+\cos\phi'\hat{\mathbf{z}}$.

It is to be noted that in the following reconstructions we have incorporated (as we have done, in fact, throughout the paper) *a priori* knowledge of the source's support; however, *a priori* knowledge of the functional form [Eq. (36)] of the source is *not* incorporated in the reconstruction algorithm.

Figure 3 depicts the spatial profile of the source $Q(\mathbf{r},t)$ used in the simulations for different, successive times of interest. It consists of a Gaussian wave packet traveling within the source's support (rectangular region) in the $\hat{\mathbf{z}}$ direction. Data for the computer simulations consisted of sampled time-domain radiation-pattern data generated synthetically from the canonical, rectangular source distribution described in Fig. 3 and collected for a finite number of uniformly spaced directions $\mathbf{s}$. The data was processed by means of the filtered backprojection formulas of Subsection 3.A. In particular, we used a discrete version of Eq. (22) for observation angles ϕ_1, $\phi_2,\ldots,\phi_n$:

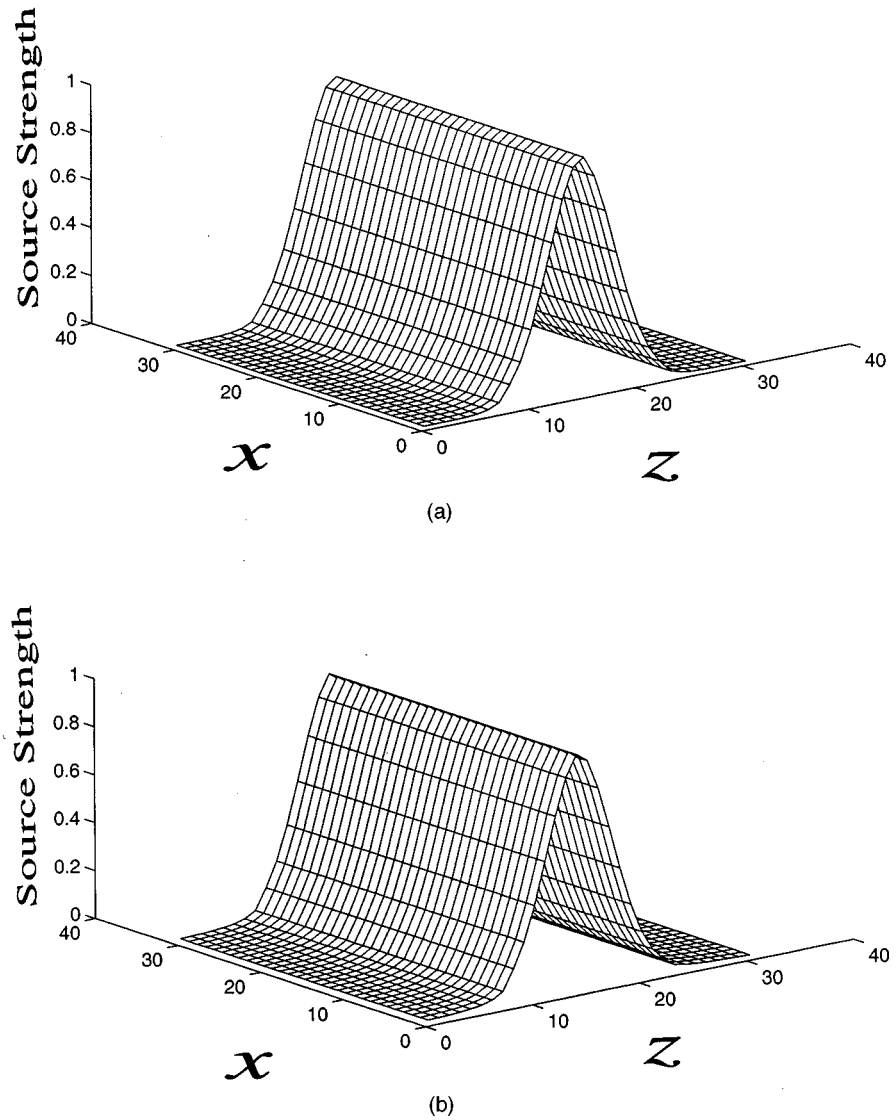

Fig. 5. Results for the time in Fig. 3(c): (a) original source spatial profile, (b) reconstructed source spatial profile obtained from the filtered backprojection algorithm.

$$(1/c)\begin{bmatrix} \Gamma(1,1) & \Gamma(1,2) & \cdot & \Gamma(1,n) \\ \Gamma(2,1) & \Gamma(2,2) & \cdot & \Gamma(2,n) \\ \cdot & \cdot & \cdot & \cdot \\ \Gamma(n,1) & \Gamma(n,2) & \cdot & \Gamma(n,n) \end{bmatrix} \begin{bmatrix} \bar{f}(1,\omega) \\ \bar{f}(2,\omega) \\ \cdot \\ \bar{f}(n,\omega) \end{bmatrix} = \begin{bmatrix} f(1,\omega) \\ f(2,\omega) \\ \cdot \\ f(n,\omega) \end{bmatrix} \quad (37)$$

where, in view of Eq. (37),

$$\Gamma(i,j) = a_x a_y \operatorname{sinc}\left[\frac{\omega a_x}{2c}(\sin\phi_i - \sin\phi_j)\right] \times \operatorname{sinc}\left[\frac{\omega a_z}{2c}(\cos\phi_i - \cos\phi_j)\right]. \quad (38)$$

Figures 4 and 5 show the results of a representative computer simulation based on time-domain radiation-pattern data provided over 50 angles. Figure 4(a) shows the spatial profile of the original source function (within its rectangular support) for the time in Fig. 3(a), and Fig. 4(b) shows the spatial profile of the reconstructed source function—evaluated at the same time—as obtained from our filtered backprojection algorithm. The agreement between the original and the reconstructed source functions is encouraging. Figure 5 shows analogous results for the time in Fig. 3(c). In all cases considered, the source-inversion technique was seen to yield good reconstructions of the original source structure.

4. TIME-DEPENDENT NONRADIATING SOURCES

It was shown in Ref. 5 that for $r > a$ the field $U(\mathbf{r}, t)$ radiated by a source $Q(\mathbf{r}, t)$ whose spatial support D is contained inside the spherical volume V: $r \leqslant a$ is given by the time-dependent multipole expansion

$$U(\mathbf{r}, t) = \frac{1}{r}\sum_{l=0}^{\infty}\sum_{m=0}^{l}\sum_{j=1,2} \epsilon_m S_{l,m}^{(j)}(\hat{\mathbf{r}})\mathcal{L}_l^{(r,t)} q_{l,m}^{(j)}(t), \quad (39)$$

where $\hat{\mathbf{r}} \equiv \mathbf{r}/r$ and where $S_{l,m}^{(j)}(\hat{\mathbf{r}})$ are the real spherical harmonics, defined as $S_{l,m}^{(1)}(\hat{\mathbf{r}}) = \mathrm{Re}\{Y_{l,m}(\hat{\mathbf{r}})\}$ and $S_{l,m}^{(2)}(\hat{\mathbf{r}}) = \mathrm{Im}\{Y_{l,m}(\hat{\mathbf{r}})\}$, Re and Im denoting the real and the imaginary parts, respectively. The constant coefficients $\epsilon_m = 1$ or 2 if $m = 0$ or $m \geqslant 1$, respectively, and

$$\mathcal{L}_l^{(r,t)} q_{l,m}^{(j)}(t) = \sum_{n=0}^{l} \frac{(l+n)!}{n!(l-n)!}\left(\frac{2r}{c}\right)^{-n} \partial_t^{-n} q_{l,m}^{(j)}(\tau), \quad (40)$$

where, as before, $\tau = t - r/c$ and $\partial_t^{-n} \equiv (\partial_t^{-1})^n$ denotes nth-order time integration, where

$$\partial_t^{-1} q_{l,m}^{(j)}(t) = \int_{-\infty}^{t} \mathrm{d}t' q_{l,m}^{(j)}(t').$$

The expansion coefficients $q_{l,m}^{(j)}(t)$ are the time-dependent multipole moments of the radiated field and are defined below.

The far field corresponds to the lowest-order term ($n = 0$) in series expansion (40) for operator $\mathcal{L}_l^{(r,t)}$. By using only this term in series expansion (40), one obtains from Eq. (39) the far-field behavior

$$U(r\mathbf{s}, t) \sim \frac{1}{r}\sum_{l=0}^{\infty}\sum_{m=0}^{l}\sum_{j=1,2} \epsilon_m S_{l,m}^{(j)}(\mathbf{s}) q_{l,m}^{(j)}(\tau) \quad \text{as} \quad r \to \infty$$

so that

$$F(\mathbf{s}, \tau) = \sum_{l=0}^{\infty}\sum_{m=0}^{l}\sum_{j=1,2} \epsilon_m S_{l,m}^{(j)}(\mathbf{s}) q_{l,m}^{(j)}(\tau). \quad (41)$$

It follows from relation (41) and the orthogonality of the real spherical harmonics $S_{l,m}^{(j)}(\mathbf{s})$ over the unit sphere S^2, i.e.,[5]

$$\int_{S^2} \mathrm{d}\mathbf{s} S_{l,m}^{(j)}(\mathbf{s}) S_{l',m'}^{(j')}(\mathbf{s}) = \delta_{l,l'}\delta_{m,m'}\delta_{j,j'}\frac{1}{\epsilon_m},$$

that

$$q_{l,m}^{(j)}(t) = \int_{S^2} \mathrm{d}\mathbf{s} F(\mathbf{s}, t) S_{l,m}^{(j)}(\mathbf{s}). \quad (42)$$

Thus the time-dependent multipole moments $q_{l,m}^{(j)}(t)$ are defined from Eq. (42) as the projections of the time-domain radiation pattern onto the set of real spherical harmonics.

By analogy with the frequency-domain treatment in Ref. 3, we define a NR source $Q_{\mathrm{NR}}(\mathbf{r}, t)$ confined within D as being a source for which the radiated energy

$$E \equiv \int_{-\infty}^{\infty} \mathrm{d}\tau \int_{S^2} \mathrm{d}\mathbf{s} |F(\mathbf{s}, \tau)|^2 = \int_{-\infty}^{\infty} \mathrm{d}t \sum_{l=0}^{\infty}\sum_{m=0}^{l}\sum_{j=1,2} \epsilon_m [q_{l,m}^{(j)}(t)]^2 = 0. \quad (43)$$

It follows immediately that a source $Q(\mathbf{r}, t)$ is NR if and only if any of the following conditions holds:

1. $q_{l,m}^{(j)}(t) = 0$ for all $l = 0, 1, \ldots$; $m = 0, 1, \ldots, l$, $j = 1, 2$, for all $t \in \Re$;
2. $F(\mathbf{s}, \tau) = 0$ for all $\tau \in \Re$ and $\mathbf{s} \in S^2$.

Conditions 1 and 2 are, in fact, the same condition since one implies the other; we have separated them to clarify the following observations. The first condition implies, in view of Eq. (39), that the radiated field itself vanishes for $r > a$, i.e., the field generated by a NR source $Q_{\mathrm{NR}}(\mathbf{r}, t)$ localized within D vanishes (at all times t) identically at all points outside V. In fact, it is widely known that the field produced by such a NR source must vanish everywhere outside D.[4,9] Also, since $F(\mathbf{s}, \tau)$ is [from Eq. (4)] determined by the fourfold Radon transform of $\rho(\boldsymbol{\mathcal{X}})$ corresponding to the hyperplane $\boldsymbol{\mathcal{X}} \cdot \boldsymbol{\mathcal{V}}_{\mathbf{s}} - c\tau/\sqrt{2} = 0$ in the 4D Radon domain or, alternatively, by the Radon projections of $\rho(\boldsymbol{\mathcal{X}})$ taken along directions $\boldsymbol{\mathcal{V}}_{\mathbf{s}}$ that lie (tangentially) on the surface of the light cone, we conclude from condition 2 that a necessary and sufficient condition for a source to be NR is the vanishing of the Radon projections of $\rho(\boldsymbol{\mathcal{X}})$ taken along those directions (see Fig. 1). Hence NR sources in the time domain are analogous to the so-called ghost (invisible) objects of CT.[23–25]

In addition to NR sources, there are sources that generate nulls in the time-domain radiation pattern [wherein

$F(\mathbf{s}, \tau) = 0$] only for certain discrete and/or continuous sets of directions $\mathbf{s}$ (corresponding to subsets of the unit sphere S^2). Sources of the latter class are of concern in the mathematical setting of inverse source problems with discrete far-field data. In particular, unlike in the full-view case, in the discrete-set case nonuniqueness arises both from sources that do not radiate at all (NR sources) and from sources that are NR only with respect to certain observation directions. The latter belong to the null space of the Radon transform corresponding to limited-view angles.[23–25] By borrowing ideas from inverse scattering[26] and CT theories,[25] one readily finds that sources of the form

$$Q(\mathbf{r}, t) = \Pi_{n=0}^{N}\left(\mathbf{s}_n \cdot \nabla + \frac{1}{c}\frac{\partial}{\partial t}\right)A(\mathbf{r}, t), \tag{44}$$

where $A(\mathbf{r}, t)$ is a differentiable function of compact spatial support D, generate far fields with nulls at the discrete set of directions $\mathbf{s}_0, \mathbf{s}_1, \ldots, \mathbf{s}_N$. By evaluating the spatial–temporal Fourier transform of the source defined by Eq. (44) for $\mathbf{k} = (\frac{\omega}{c})\mathbf{s}$, one finds that

$$\int_{-\infty}^{\infty} \mathrm{d}t \exp(i\omega t) \int_D \mathrm{d}^3 r \exp(-i\omega \mathbf{s} \cdot \mathbf{r}/c) Q(\mathbf{r}, t)$$

$$= \left[\Pi_{n=0}^{N} i\frac{\omega}{c}(\mathbf{s}_n \cdot \mathbf{s} - 1)\right] \int_{-\infty}^{\infty} \mathrm{d}t \exp(i\omega t)$$

$$\times \int_D \mathrm{d}^3 r \exp(-i\omega \mathbf{s} \cdot \mathbf{r}/c) A(\mathbf{r}, t),$$

which is seen to vanish for $\mathbf{s} = \mathbf{s}_0, \mathbf{s} = \mathbf{s}_1, \ldots, \mathbf{s} = \mathbf{s}_N$, thereby confirming the vanishing of the far fields at those observation directions.

We conclude this section with an orthogonality relation between NR sources and solutions of the homogeneous wave equation that leads to a new definition of NR sources in the time domain. The time-harmonic counterpart of the relation in question was derived first in Ref. 27 and is generalized here to arbitrary time dependence.

Let $U_{\mathrm{R}}(\mathbf{r}, t)$ and $U_{\mathrm{NR}}(\mathbf{r}, t)$ be the real-valued fields that are produced by a radiating and a NR source $Q_{\mathrm{R}}(\mathbf{r}, t)$ and $Q_{\mathrm{NR}}(\mathbf{r}, t)$, respectively, and that obey the inhomogeneous wave equations

$$\left(\nabla^2 - \frac{1}{c^2}\frac{\partial^2}{\partial t^2}\right)U_{\mathrm{R}}(\mathbf{r}, t) = -4\pi Q_R(\mathbf{r}, t), \tag{45}$$

$$\left(\nabla^2 - \frac{1}{c^2}\frac{\partial^2}{\partial t^2}\right)U_{\mathrm{NR}}(\mathbf{r}, t) = -4\pi Q_{\mathrm{NR}}(\mathbf{r}, t). \tag{46}$$

Let $Q_{\mathrm{R}}(\mathbf{r}, t)$ and $Q_{\mathrm{NR}}(\mathbf{r}, t)$ be localized, respectively, in disjoint simply connected spatial–temporal domains $\mathcal{D}_{\mathrm{R}}$ and $\mathcal{D}$. By multiplying Eq. (45) by $U_{\mathrm{NR}}(\mathbf{r}, t)$ and Eq. (46) by $U_{\mathrm{R}}(\mathbf{r}, t)$, we obtain

$$U_{\mathrm{NR}}(\mathbf{r}, t)\left(\nabla^2 - \frac{1}{c^2}\frac{\partial^2}{\partial t^2}\right)U_{\mathrm{R}}(\mathbf{r}, t)$$

$$= -4\pi U_{\mathrm{NR}}(\mathbf{r}, t) Q_{\mathrm{R}}(\mathbf{r}, t), \tag{47}$$

$$U_{\mathrm{R}}(\mathbf{r}, t)\left(\nabla^2 - \frac{1}{c^2}\frac{\partial^2}{\partial t^2}\right)U_{\mathrm{NR}}(\mathbf{r}, t)$$

$$= -4\pi U_{\mathrm{R}}(\mathbf{r}, t) Q_{\mathrm{NR}}(\mathbf{r}, t). \tag{48}$$

By subtracting Eq. (47) from Eq. (48) and integrating both sides of the resulting equation over space–time, one obtains by means of Green's theorem

$$\int_{\mathcal{D}} \mathrm{d}t \mathrm{d}^3 r U_{\mathrm{R}}(\mathbf{r}, t) Q_{\mathrm{NR}}(\mathbf{r}, t) = 0, \tag{49}$$

where we have used the fact that $U_{\mathrm{NR}}(\mathbf{r}, t)$ vanishes outside the spatial–temporal support $\mathcal{D}$. By noting that

$$\left(\nabla^2 - \frac{1}{c^2}\frac{\partial^2}{\partial t^2}\right)U_{\mathrm{R}}(\mathbf{r}, t) = 0 \qquad \text{if } (\mathbf{r}, t) \in \mathcal{D}, \tag{50}$$

one concludes from Eq. (49) that NR sources localized in the spatial–temporal region $\mathcal{D}$ are orthogonal to solutions of the homogeneous wave equation inside $\mathcal{D}$.

Finally, we conclude by showing that a source of spatial–temporal support $\mathcal{D}$ is NR if and only if it obeys orthogonality relation (49) with respect to any solution of homogeneous wave equation (50) inside $\mathcal{D}$. The analysis above reveals that this condition is necessary. We need to show only sufficiency. This is accomplished readily by noting that the causal Green function

$$G(\mathbf{r} - \mathbf{r}', t - t') = \delta(t' + |\mathbf{r} - \mathbf{r}'|/c - t)/|\mathbf{r} - \mathbf{r}'|$$

obeys

$$\left(\nabla^2 - \frac{1}{c^2}\frac{\partial^2}{\partial t^2}\right)G(\mathbf{r} - \mathbf{r}', t - t') = 0$$

if the space–time point $(\mathbf{r}, t)$ is inside $\mathcal{D}$ and $(\mathbf{r}', t')$ is outside $\mathcal{D}$. Then, by using $U_{\mathrm{R}}(\mathbf{r}, t) = G(\mathbf{r} - \mathbf{r}', t - t')$ (for fixed $(\mathbf{r}', t')$ outside $\mathcal{D}$) in Eq. (49), we find that

$$\int_{\mathcal{D}} \mathrm{d}t' \mathrm{d}^3 r' G(\mathbf{r} - \mathbf{r}', t - t') Q_{\mathrm{NR}}(\mathbf{r}', t') = 0$$

$$\text{if } (\mathbf{r}, t) \notin \mathcal{D}. \tag{51}$$

One concludes from Eq. (51) that $Q_{\mathrm{NR}}(\mathbf{r}, t)$ must vanish at all space–time points outside the spatial support of $Q_{\mathrm{NR}}(\mathbf{r}, t)$, which confirms the NR nature of $Q_{\mathrm{NR}}(\mathbf{r}, t)$. We have thus obtained a new definition of NR sources in the time domain based on orthogonality relation (49).

5. CONCLUSION

We have presented a new treatment of the (time-dependent) inverse source problem with far-field data that makes use of standard linear operator theory and a Radon-transform representation of the time-domain radiation pattern. In Subsection 3.A we derived a new filtered backprojectionlike method to reconstruct the ME source consistent with prescribed far-field data. Among other results, ME sources contained in a spatial–temporal domain $\mathcal{D}$ were found to obey a homogeneous wave equation in the interior of $\mathcal{D}$. The general theory in Subsection 3.A was developed further in Subsection 3.B, where we addressed the canonical example of a source localized within a spherical shell. In Subsection 3.C we

presented the results of a numerical simulation that illustrated the general theory. In Section 4 we characterized NR sources in the time domain by using time-dependent multipoles. We found that NR sources in the time domain are analogous to the so-called ghost objects that arise in the formalism of the limited-view CT problem. An orthogonality relation for NR sources derived under time-harmonic conditions in a previous paper,[27] was generalized to the time domain and used as the basis for a new definition of a NR source having a given spatial–temporal support.

ACKNOWLEDGMENTS

This work was supported in part by the Air Force Office of Scientific Research, Air Force Materials Command, USAF, under grants F49620-93-1-0093 and F49620-96-1-0039. E. A. Marengo acknowledges partial support from the Center for Electromagnetics Research at Northeastern University.

REFERENCES

1. J. D. Jackson, *Classical Electrodynamics*, 2nd ed. (Wiley, New York, 1975).
2. N. Bleistein and J. K. Cohen, "Nonuniqueness in the inverse source problem in acoustics and electromagnetics," J. Math. Phys. **18**, 194–201 (1977).
3. A. J. Devaney and E. Wolf, "Radiating and nonradiating classical current distributions and the fields they generate," Phys. Rev. D **8**, 1044–1047 (1973).
4. A. J. Devaney and R. P. Porter, "Holography and the inverse source problem. Part II: inhomogeneous media," J. Opt. Soc. Am. A **2**, 2006–2011 (1985).
5. E. Heyman and A. J. Devaney, "Time-dependent multipoles and their application for radiation from volume source distributions," J. Math. Phys. **37**, 682–692 (1996).
6. P. R. Smith, T. M. Peters, and R. H. T. Bates, "Image reconstruction from finite number of projections," J. Phys. A Math. Nucl. Gen. **6**, 361–382 (1973).
7. A. K. Louis, "Incomplete data problems in x-ray computerized tomography. I. Singular value decomposition of the limited angle transform," Numer. Math. **48**, 251–262 (1986).
8. A. D. Yaghjian and T. B. Hansen, "Time-domain far fields," J. Appl. Phys. **79**, 2822–2830 (1996).
9. F. G. Friedlander, "An inverse problem for radiation fields," Proc. London Math. Soc. **3**, 551–576 (1973).
10. M. Bertero, C. De Mol, and E. R. Pike, "Linear inverse problems with discrete data. I: general formulation and singular system analysis," Inverse Probl. **1**, 301–330 (1985).
11. I. J. LaHaie, "The inverse source problem for three-dimensional partially coherent sources and fields," J. Opt. Soc. Am. A **2**, 35–45 (1985).
12. H. E. Moses, "Solution of Maxwell's equations in terms of a spinor notation: the direct and inverse problem," Phys. Rev. **113**, 1670–1679 (1959).
13. H. E. Moses, "The time-dependent inverse source problem for the acoustic and electromagnetic equations in the one- and three-dimensional cases," J. Math. Phys. **25**, 1905–1923 (1984).
14. R. W. Deming and A. J. Devaney, "A filtered backpropagation algorithm for GPR," J. Env. Eng. Geo. **0**, 113–123 (1996).
15. S. R. Deans, *The Radon Transform and Some of Its Applications* (Wiley, New York, 1983).
16. D. N. Ghosh Roy, *Methods of Inverse Problems in Physics*, 2nd ed. (CRC Press, Boca Raton, Fla., 1991).
17. M. Bertero, "Linear inverse and ill-posed problems," in P. W. Hawkes, ed., *Advances in Electronics and Electron Physics* (Academic, New York, 1989), Vol. 75, pp. 1–120.
18. R. P. Porter and A. J. Devaney, "Generalized holography and computational solutions to inverse source problems," J. Opt. Soc. Am. **72**, 1707–1713 (1982).
19. E. A. Marengo, A. J. Devaney, and E. Heyman, "Analysis and characterization of ultrawideband, scalar volume sources and the fields they radiate," IEEE Trans. Antennas Propag. **45**, 1098–1107 (1997).
20. E. A. Marengo, A. J. Devaney, and E. Heyman, "Analysis and characterization of ultrawideband, scalar volume sources and the fields they radiate: Part II—square pulse excitation," IEEE Trans. Antennas Propag. **46**, 243–250 (1998).
21. K. T. Ladas and A. J. Devaney, "Generalized ART algorithm for diffraction tomography," Inverse Probl. **7**, 109–125 (1991).
22. G. Arfken, *Mathematical Methods for Physicists*, 3rd ed. (Academic, San Diego, Calif., 1985).
23. A. K. Louis, "Ghosts in tomography—The null space of the Radon transform," Math. Methods Appl. Sci. **3**, 1–10 (1981).
24. A. K. Louis, "Orthogonal function series expansions and the null space of the Radon transform," SIAM J. Math. Anal. **15**, 621–633 (1984).
25. K. T. Smith, D. C. Solmon, and S. L. Wagner, "Practical and mathematical aspects of the problem of reconstructing objects from radiographs," Bull. Am. Math. Soc. **83**, 1227–1270 (1977).
26. A. J. Devaney, "Nonuniqueness in the inverse scattering problem," J. Math. Phys. **19**, 1526–1531 (1978).
27. K. Kim and E. Wolf, "Non-radiating monochromatic sources and their fields," Opt. Commun. **59**, 1–6 (1986).